

Feasibility studies for nucleon structure measurements with PANDA

Ermias Atomssa^{1,a} and Binsong Ma¹
for the PANDA Collaboration

¹*Institut de Physique Nucléaire d'Orsay, 91406, Orsay, France*

Abstract. The study of nucleon structure is one of the main physics goals of PANDA to be built at the FAIR accelerator complex. The excellent particle identification performance of the PANDA detector will enable measurements of exclusive channels $\bar{p}p \rightarrow e^+e^-$ and $\bar{p}p \rightarrow \pi^0 J/\psi \rightarrow \pi^0 e^+e^-$ to extract the electromagnetic form factors of protons and π -nucleon Transition Distribution Amplitudes (π - N TDAs). After a brief description of the PANDA apparatus and a method to handle momentum resolution degradation due to Bremsstrahlung, the physics of π - N TDAs is discussed. An estimate for the expected signal to background ratio for $\bar{p}p \rightarrow \pi^0 J/\psi \rightarrow \pi^0 e^+e^-$ that takes into account the main background source is given.

1 PANDA experimental setup

The PANDA detector [1] is a multi-purpose experiment to be installed at the Facility for Antiproton and Ion Research (FAIR). It is currently under active development and will exploit the possibilities offered by a secondary antiproton beam of 1.5 to 15 GeV/c that will be available at the High Energy Storage Ring (HESR) of FAIR. The physics goals of PANDA span a very wide range of interests, but the focus here will be the study of nucleon structure (section 3). Due to the large cross-section of hadronic background involved, nucleon structure measurements require excellent performance in terms of particle identification (PID) and momentum resolution. The main detector sub-components for this purpose will be discussed briefly below.

The PANDA tracking system is composed of a silicon pixel based Multiplicity Vertex Detector (MVD) [2], a Straw Tube Tracker (STT) [3] and a Gas Electron Multiplier (GEM) tracker [1]. In addition to momentum reconstruction of charged particles with a resolution of 1.6% at 1 GeV/c, the tracking system will also provide PID information in the form of 24 dE/dx measurements in the individual layers of the STT. Due to the sizable material budget, in particular from the MVD, electrons have a high probability to lose significant energy through Bremsstrahlung photon emission, leading to a degradation of their momentum resolution. A method to mitigate the loss of resolution by identifying Bremsstrahlung photons and adding back their energy to the electron momentum is proposed in section 2.

The PbWO₄ based PANDA electromagnetic calorimeter (EMC) [4] is designed to perform with large dynamic range ($\gtrsim 3$ MeV and $\lesssim 10$ GeV) and high resolution ($\sigma(E)/E \approx 1\% \oplus 2\%/\sqrt{E(\text{GeV})}$),

^ae-mail: atomssa@ipno.in2p3.fr

and operate under a large magnetic field strength and significant radiation dose. In addition to the reconstruction of photons and neutral mesons that decay into a pair of photons, the EMC is also an important component in electron identification. The correlation between the momentum from tracking and energy from the EMC provides a good separation between charged pions and electrons. However at low momenta, the separation power is worse.

Electron identification in the low momentum region is covered by the DIRC (detection of internally reflected Čerenkov light) [1]. The DIRC is a Čerenkov detector that measures the photon emission angle which has characteristic momentum dependence for different particles. The global PID works by combining the information from DIRC, EMC and STT. It is possible to achieve a mis-identification rate of single charged pions of the order of $\approx 10^{-4}$ while keeping electron efficiency above $\approx 70\%$ in all of the relevant momentum range above 500 MeV. Below 500 MeV, the efficiency for electrons drops sharply to about 10%.

2 Bremsstrahlung correction

The geometry of the PANDA detector, where most of the material budget is concentrated in the first few layers of tracking (MVD), and the excellent dynamic range and resolution of the EMC will allow for an event by event handling of Bremsstrahlung energy loss correction. This is accomplished by a method [5] that exploits the fact that the photons are emitted in a very narrow cone around the electron track. The result is that the Bremsstrahlung photon cluster positions in the EMC are closely correlated in space to the cluster of the electron from which they originate. The method identifies both separate photon clusters (using proximity cuts) and merged clusters (using shape analysis), to estimate the amount of energy to add back to the reconstructed momentum of the electron tracks. Using this method, it is possible to improve the momentum resolution of electron reconstruction. This is illustrated in Fig. 1 where the invariant mass distributions of e^+e^- are shown for full simulations of two channels of particular interest to nucleon structure measurements: $\bar{p}p \rightarrow e^+e^-$ and $\bar{p}p \rightarrow \pi^0 J/\psi \rightarrow \pi^0 e^+e^-$. In both cases, the use of the Bremsstrahlung correction method improves significantly the amount of signal within the cut windows (more than 60% increase in efficiency).

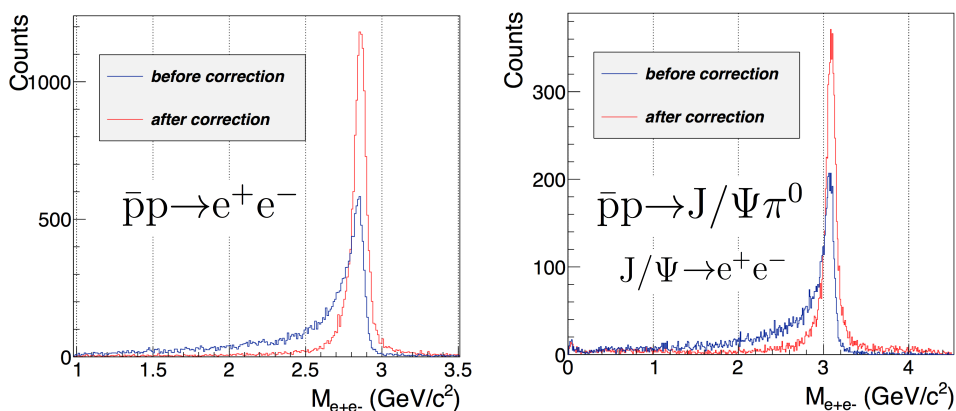


Figure 1. Improvement to the invariant mass resolutions of $\bar{p}p \rightarrow e^+e^-$ (left panel) and $\bar{p}p \rightarrow \pi^0 J/\psi \rightarrow \pi^0 e^+e^-$ (right panel) by applying the Bremsstrahlung correction method.

3 Nucleon structure measurements

The main nucleon structure measurements that are planned with PANDA are the time-like electric $G_E(q^2)$ and magnetic $G_M(q^2)$ form factors of protons in $\bar{p}p \rightarrow e^+e^-$ reactions and the π -nucleon Transition Distribution Amplitudes (TDAs) in $\bar{p}p \rightarrow \pi^0 J/\psi \rightarrow \pi^0 e^+e^-$ and $\bar{p}p \rightarrow \pi^0 \gamma^* \rightarrow \pi^0 e^+e^-$ reactions. Due to lack of space, the discussion below will focus on π - N TDAs. Consult [6] for a review on electromagnetic form factors.

TDAs are functions that appear in the factorized calculation of the cross-section of hard exclusive processes. They capture a part of the amplitude that is not calculable perturbatively, and thus represent the long distance components that encode information about the structure of hadrons. The validity of factorization requires a hard scale that is usually taken to be the virtuality of the exchanged photon. The main interest of TDAs is that they are universal, and thus can be constrained in a given channel and can be used in cross-section calculation of a related channel.

In particular, π - N TDAs arise in cross-section calculations of virtual photon or J/ψ production with associated π^0 ($\bar{p}p \rightarrow \pi^0 \gamma^* \rightarrow \pi^0 e^+e^-$ [7] and $\bar{p}p \rightarrow \pi^0 J/\psi \rightarrow \pi^0 e^+e^-$ [8]) as well as backward pion electroproduction ($\gamma^* N \rightarrow \pi N$) [9]. They give information about the pionic component of nucleon wave function. As shown in Fig. 2, for the case of $\bar{p}p \rightarrow \pi^0 J/\psi \rightarrow \pi^0 e^+e^-$, the cross-section involves a hard component, J/ψ formation, that is calculable perturbatively using the same formalism as for the decay of J/ψ into $\bar{p}p$. The distribution amplitudes (DA) of hadrons are another long distance component that can be constrained separately using data on the $J/\psi \rightarrow \bar{p}p$ partial decay width.

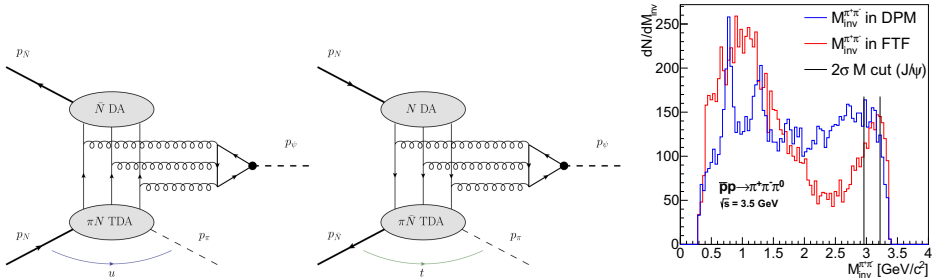


Figure 2. Left: Feynman diagrams used in the calculation of the $\bar{p}p \rightarrow \pi^0 J/\psi \rightarrow \pi^0 e^+e^-$ cross-section in a π - N TDA formalism for the backward kinematics at small $u = (p_\pi - p_N)^2 \approx 0$ (left most) and the forward kinematics at small $t = (p_\pi - p_{\bar{N}})^2 \approx 0$ (middle). Right: Invariant mass distribution of $\pi^+ \pi^-$ pairs from DPM and FTF hadronic interaction event generators. Two lines correspond to typical cuts around the J/ψ mass.

In the formalism presented in [8], in addition to the hard scale requirement for factorization, which is satisfied by taking the scale at the J/ψ mass, the validity of the calculation is guaranteed only in two kinematic domains: small u (backward kinematics, π^0 in the direction of the nucleon) probing the π - N TDAs and small t (forward kinematics, π^0 in the direction of the anti-nucleon) probing the π - \bar{N} TDAs. The cross-section estimates from the TDA formalism of 0.2 nb given in [8] (t and u channels combined) agree with the only available data on $\bar{p}p \rightarrow \pi^0 J/\psi \rightarrow \pi^0 e^+e^-$ from Fermilab [10] at a CM energy close to the h_c resonance mass ($\sqrt{s} = 3.25$ GeV). One should note that the angular distribution of the emission of π^0 can in principle be used to disentangle between this mechanism and alternatives proposed in the literature, such as the effective Lagrangian approach of [11]. However this requires a high statistics measurement which may not be easily achievable even with the maximum design luminosity of PANDA.

4 Feasibility of π - N TDA measurements

The main background for $\bar{p}p \rightarrow \pi^0 J/\psi \rightarrow \pi^0 e^+ e^-$ comes from the three pion production $\bar{p}p \rightarrow \pi^0 \pi^+ \pi^-$ which has a very similar topology and kinematics as the signal reaction. The rate of this reaction is sufficiently well known from previous measurements [12–14]. Other sources are either very easy to reject using kinematics (for example two π^0 production) or have too low branching ratios (J/ψ decay to $\pi^+ \pi^-$) to be of concern. At around the mass of the h_c the closest data points are at \bar{p} lab momenta of 4.6 GeV/c and 5.7 GeV/c. The interpolated cross-section of 0.2 ± 0.05 mb is used as a starting point for the estimation. This cross-section is a factor of $\approx 1.7 \times 10^7$ above the signal taking into account J/ψ to $e^+ e^-$ branching ratio of 5.94%. It therefore imposes very stringent requirements on electron identification and pion rejection.

Using a parametrization of the electron efficiency and charged pions mis-identification rate discussed in section 1 as well as a parametrization of the π^0 reconstruction efficiency, we obtain a total PID efficiency for $\bar{p}p \rightarrow \pi^0 J/\psi \rightarrow \pi^0 e^+ e^-$ of $\varepsilon_{PID}^{SIG} \approx 40\%$ and a mis-id rate for the $\bar{p}p \rightarrow \pi^0 \pi^+ \pi^-$ of $\varepsilon_{MIS-ID}^{BG} \approx 7.3 \times 10^{-8}$. Track reconstruction efficiencies cancel out between signal and background. In addition to PID cuts, one can exploit the fact that the J/ψ mass resonance is very narrow. Applying a cut of $2.96 < M_{inv}[\text{GeV}/c^2] < 3.22$ will keep roughly $\varepsilon_{m-cut}^{SIG} \approx 64\%$ of the J/ψ peak while rejecting more than 90% of $\bar{p}p \rightarrow \pi^0 \pi^+ \pi^-$ events ($\varepsilon_{m-cut}^{BG} \approx 10\%$). This can be seen in the right panel of Fig. 2, where the invariant mass of the $\pi^+ \pi^-$ pair from simulation using two independent event generators based on string fragmentation (DPM [15] and FTF [16]) are plotted for antiproton momentum of 5.513 GeV/c. Combining these numbers leads to an estimated S/B of about ≈ 2 –3. This background will be measurable with high precision and sufficiently low to enable subtraction or direct fitting of the J/ψ peak in the mass distribution. Assuming an integrated luminosity of 2 fb^{-1} from four months worth of data taking at full design luminosity, the expected counting rate of about 6600 of signal events in the combined t and u channels will be comfortable to extract differential cross-section distributions with reasonable uncertainties.

References

- [1] W. Erni, et al. (PANDA Collaboration), ArXiv e-prints (2009), 0903.3905
- [2] W. Erni, et al. (PANDA Collaboration), ArXiv e-prints (2012), 1207.6581
- [3] W. Erni, et al. (PANDA Collaboration), ArXiv e-prints (2012), 1205.5441
- [4] W. Erni, et al. (PANDA Collaboration), ArXiv e-prints (2008), 0810.1216
- [5] B. Ma (for the PANDA Collaboration), J. Phys. Conf. Ser. **503**, 012008 (2014)
- [6] A. Denig, G. Salme, Prog. Part. Nucl. Phys. **68**, 113 (2013), 1210.4689
- [7] J.P. Lansberg, et al., Phys. Rev. D **86**, 114033 (2012)
- [8] B. Pire, et al., Phys. Lett. B **724**, 99 (2013)
- [9] J.P. Lansberg, et al., Phys. Rev. D **85**, 054021 (2012)
- [10] M. Andreotti et al., Phys. Rev. **D72**, 032001 (2005)
- [11] J. Van de Wiele, S. Ong, Eur. Phys. J. **C73**, 2640 (2013)
- [12] V. Flaminio, et al. (High-Energy Reactions Analysis Group), *Compilation of cross-sections* (CERN, Geneva, 1984), updated version of CERN HERA 79-03
- [13] D. Everett, et al., Nucl. Phys. B **73**, 449 (1974)
- [14] H. Braun, et al., Nucl. Phys. B **95**, 481 (1975)
- [15] A. Capella, U. Sukhatme, C.I. Tan, J. Tran Thanh Van, Phys. Rep. **236**, 225 (1994)
- [16] B. Andersson, G. Gustafson, H. Pi, Z. Phys. **C57**, 485 (1993)